AAPS PharmSciTech, Vol. 9, No. 1, March 2008 (© 2008)
DOI: 10.1208/s12249-008-9036-x

Research Article

Intracellular Delivery of Nanoparticles of an Antiasthmatic Drug

Naazneen Surti,[1] Sachin Naik,[1] Tamishraha Bagchi,[2] B. S. Dwarkanath,[3] and Ambikanandan Misra[1,4]

Received 4 August 2007; accepted 4 January 2008; published online 7 February 2008

Abstract. The aim of the investigation was to prepare and characterize wheat germ agglutinin(WGA)-conjugated poly(D,L-lactic-*co*-glycolic) acid nanoparticles encapsulating mometasone furoate (MF) as a model drug and assess changes in its fate in terms of cellular interactions. MF loaded nanoparticles were prepared using emulsion–solvent evaporation technique. WGA-conjugation was done by carbodiimide coupling method. The nanoparticles were characterized for size, zeta potential, entrapment efficiency and *in-vitro* drug release. The intracellular uptake of nanoparticles, drug cellular levels, and anti-proliferative activity studies of wheat germ agglutinin-conjugated and unconjugated nanoparticles were assessed on alveolar epithelial (A549) cells to establish cellular interactions. Prepared nanoparticles were spherical with 10–15 μg/mg of WGA conjugated on nanoparticles. The size of nanoparticles increased after conjugation and drug entrapment and zeta potential reduced from 78±5.5% to 60±2.5% and −15.3±1.9 to −2.59±2.1 mV respectively after conjugation. From the cellular drug concentration–time plot, AUC was found to be 0.4745, 0.6791 and 1.24 for MF, MF-nanoparticles and wheat germ agglutinin-MF-nanoparticles respectively. The *in-vitro* antiproliferative activity was improved and prolonged significantly after wheat germ agglutinin-conjugation. The results conclusively demonstrate improved availability and efficacy of antiasthmatic drug in alveolar epithelial cell lines. Hence, a drug once formulated as mucoadhesive nanoparticles and incorporated in dry powder inhaler formulation may be used for targeting any segment of lungs for more improved therapeutic response in other lung disorders as well.

KEY WORDS: intracellular levels; mometasone furoate; nanoparticles; poly(D; L-lactic-*co*-glycolic) acid; sustained delivery; wheat germ agglutinin.

INTRODUCTION

The therapeutic efficacy of drugs, which have their receptors located in the cytoplasm, depends on the dose and duration of availability of these drugs in the cytoplasm. For many therapeutic agents, the intracellular drug levels are maintained transiently when used as solution, and hence, the therapeutic effect is seen only for a short duration (1). Hence, a delivery system that could slowly release the drug intracellularly would enhance the therapeutic efficacy of the drug as well as could sustain its therapeutic effect.

Nanoparticles are submicron-sized polymeric colloidal particles with a therapeutic agent of interest encapsulated within their polymeric matrix or adsorbed or conjugated onto the surface. Among the polymers used for the preparation of nanoparticles, poly(D,L-lactic-*co*-glycolic) acid (PLGA) is highly preferred because it is biodegradable and biocompatible. The drug entrapped in PLGA matrix is released at a sustained rate through diffusion of the drug in the polymer matrix and by degradation of the polymer matrix (2). Drug loaded nanoparticles formulated from PLGA have been shown to be internalized by the cells and retained intracellularly, releasing drug for extended period of time (3). PLGA nanoparticles have also been shown to rapidly escape the endo-lysosomal compartment and be released into the cytosol (4).

Lectins are a family of natural nonenzymatic proteins/glycoproteins that have cytoadhesive and cytoinvasive properties. Lectins specifically recognize and bind with carbohydrate residues on cell surface to initiate vesicular transport processes of cells (5). Because of their specificity and their resistance to protease degradation, several lectins have been explored for pharmaceutical applications. The wheat germ agglutinin (WGA) from *Triticum vulgare* is being used widely in drug delivery research because it is widely characterized and one of the least immunogenic lectins (6). It binds specifically to *N*-acetyl-D-glucosamine residues located at the surface of alveolar epithelium (7). Specific binding followed by internalization of WGA has also been demonstrated in intestinal and alveolar epithelium (8).

Mometasone furoate (MF) was taken as a model drug because it is one of the newer and more potent inhaled corticosteroids used in the management of persistent mild-to-moderate asthma in adults and adolescents. It has been

[1] Pharmacy Department, Faculty of Technology and Engineering, Kalabhavan, The Maharaja Sayajirao University of Baroda, Vadodara 390001, Gujarat, India.
[2] Department of Microbiology and Biotechnology Centre, Faculty of Science, The Maharaja Sayajirao University of Baroda, Sayajigunj, Vadodara 390002, India.
[3] Institute of Nuclear Medicine and Allied Sciences, New Delhi, India.
[4] To whom correspondence should be addressed. (e-mail: misraan@hotmail.com)

shown to inhibit sulfidoleukotriene production (9). The sulfidoleukotriene are potent eicosanoid mediators which play an important role in the pathophysiology of allergic disease (10). Production of these arachidonic acid metabolites is increased in both atopic asthmatic (11) and allergic rhinitic (12) patients. In addition, the effects of the sulfidoleukotrienes have been shown to precipitate pathologic changes similar to those found in asthma, both *in vitro* and *in vivo* (11). Mometasone furoate has also been shown to be a potent inhibitor of the *in vitro* production of three inflammatory cytokines, IL-1 (1), IL-6, and TNF-alpha (13).

Asthma being a chronic disorder there is a need to sustain the inhibition of factors leading to asthma. Therefore the aim of this investigation was to prepare nanoparticles of an antiasthmatic drug, mometasone furoate, conjugate WGA onto the surface of nanoparticles and evaluate them for sustained intracellular concentrations using alveolar epithelial cells (A549).

MATERIALS AND METHODS

Materials

PLGA, (lactide/glycolide ratio 50:50, inherent viscosity 0.45 dl/g) was obtained as a gift sample from Boehringer Ingelheim, Germany. Mometasone furoate was obtained as a gift sample from Alembic chemicals, limited, Baroda. Polyvinyl alcohol (PVA; MW 125,000; hydrolyzed 87–89%) was purchased from S.D. fine Chemicals, India. WGA and Bichinconinic acid protein Assay Kit were obtained from Banglore Genei, India. A549 cells were obtained from National Center for Cell Sciences, Pune, India. Dulbecco's modified Eagle medium (DMEM), sodium bicarbonate, streptomycin–penicillin solution, fetal bovine serum, fluorescein di-acetate and Hank's balanced salt solution, trypsin-ethylene diamine tetra acetic acid, propidium iodide and ribonuclease A were purchased from Sigma Chemical Co., USA. 1-ethyl-3(3-dimethylaminopropyl) carbodiimide hydrochloride (EDAC), *N*-hydroxy-succinimide (NHS), glycine, *N*-(2-hydroxyethyl) piperazine-*N*′-(2-ethanesulfonic acid; HEPES), Sodium dodecyl sulphate were purchased from National Chemicals, India. Methylene chloride, methanol and glacial acetic acid obtained from Loba Chemicals, India were of HPLC grade. Tissue culture flasks and 24-well plates were obtained from Tarsons Ltd, India. All the other reagents used for the present study were of analytical grade.

Methods

Preparation of Mometasone Furoate-PLGA Nanoparticles

Mometasone furoate encapsulated PLGA nanoparticles were prepared using emulsion–solvent evaporation technique (14). Briefly, Mometasone furoate and polymer (different drug/polymer ratios) were added to dichloromethane, and the contents were allowed to stand at room temperature for 30 to 45 min with occasional stirring to allow complete solubilization of the drug and the polymer. This solution was poured into an aqueous PVA solution (0.5–2.0% *w*/*v*) and the resulting mixture was stirred with the help of high speed homogenizer (Ultra-turrax, T-25, Ultrapure Scientific, Mumbai) to get a primary *O*/*W* emulsion. The primary emulsion was passed through high pressure homogenizer (Emulsiflex, C5, Avestin, Canada) for three cycles at 15,000 psi pressure. The homogenized O/W emulsion was immediately added drop-wise to an aqueous PVA solution (0.5–2.0% *w*/*v*) and the contents were stirred overnight with a magnetic stirrer (Remi Equipments, Mumbai) to evaporate the methylene chloride. Nanoparticles were recovered by centrifugation for 30 min at 25,000 rpm, washed two times with distilled water to remove unentrapped drug and PVA, and then lyophilized for 24 h.

WGA-Conjugation of Mometasone Furoate-PLGA Nanoparticles

WGA was conjugated to mometasone furoate-PLGA nanoparticle surface by the two-step carbodiimide process, which involved the activation of the carboxyl groups on the particle surface by an EDAC/NHS mixture (15), followed by binding of the activated carboxyl groups to the amino groups in WGA. Briefly, 1.0 ml, 7.0% *w*/*v* solution of EDAC and 1.0 ml of 0.3% *w*/*v* NHS solution in 20 mM HEPES/NaOH buffer, pH 7.0, were added to a suspension of 10 mg nanoparticles in the same buffer. After 2 h of incubation at room temperature, excess EDAC and NHS were removed by centrifugation. The supernatant was discarded and the pellet was resuspended in 1.0 ml of 20 mM HEPES/NaOH buffer, pH 7.0. WGA solution, in 20 mM HEPES/NaOH buffer, pH 7.0, equivalent to 200 μg was added to the NP suspension and incubated for 18 h. Excess WGA was removed by centrifugation. To saturate the free coupling sites 1.0 ml of 20% glycine solution in 20 mM HEPES/NaOH buffer, pH 7.4 was added and incubated for 1 h. Finally, the particles were washed with 20 mM HEPES/NaOH buffer, pH 7.0 and lyophilized for 24 h (16). To estimate the amount of WGA conjugated onto the surface of mometasone furoate-nanoparticles, the amount of WGA in the supernatant and the washings was subtracted from the amount of WGA taken for conjugation. This was also confirmed by lysing the lyophilized WGA-nanoparticles with 5% SDS/0.1 M NaOH and determining the protein content by Bichinconinic acid protein assay method.

Characterization of Nanoparticles

Mometasone furoate-PLGA nanoparticles and WGA conjugated mometasone furoate-PLGA nanoparticles were characterized for the following parameters:

Particle size and zeta potential. A 2.0 mg sample of nanoparticles was suspended in distilled water, and the particle size and zeta potential were measured using the principle of laser light scattering with zeta sizer (Nano-ZS, Malvern Instruments, UK).

Entrapment efficiency. The entrapment efficiency of Mometasone furoate in the nanoparticles was determined by extracting and quantifying the encapsulated mometasone furoate (14). Briefly, 2 mg of nanoparticles were added to 5 ml of methylene chloride and subjected to shaking at room temperature for 16 h to ensure complete dissolution of the particles. The resulting solution was evaporated to dryness,

and the dried residue was reconstituted with 1 ml of mobile phase. The reconstituted solution was centrifuged and the supernatant was injected into the HPLC column. The percent entrapment efficiency (% EE) was calculated using the following expression.

$$\%EE = (\text{Amount of drug in the nanoparticles}/\text{drug added in the formulation}) \times 100$$

In-vitro drug release. A suspension of nanoparticles containing 500 μg mometasone furoate, in phosphate-buffered saline at 37°C, was placed in a dialysis bag and suspended in 15 ml PBS (pH 7.4). Sampling was done at predetermined time intervals and volume was adjusted by replacing with fresh PBS. To determine the amount of mometasone furoate in the samples, the samples were extracted with methylene chloride for 30 min. The methylene chloride was evaporated and the residue reconstituted with the mobile phase, centrifuged and injected into the HPLC column. The release of mometasone furoate from plain mometasone furoate suspension was used as a control.

Surface morphology. The morphology of the nanoparticles was analyzed using EDAX (Energy dispersion analysis by X-ray) Scanning Electron Microscopy (ESEM). Aqueous nanoparticle suspensions were layered on the SEM stubs, and allowed to dry at room temperature. Samples were then observed with Phillips SEM 51 S set at 10 kV.

Cell Culture

Alveolar epithelial cells (A549) were maintained on Dulbecco's modified eagle medium, supplemented with sodium bicarbonate, fetal bovine serum and streptomycin–penicillin solution. All the incubations were performed at 37°C and 5% CO_2.

Cellular Uptake

To visualize cellular uptake, A549 cells (passage 82) were seeded on a coverslip placed in 35 mm petri dishes at a cell density of 0.1×10^6 cells per petri dish and allowed to attach overnight. The cells were treated with WGA conjugated and unconjugated nanoparticles loaded with 6-coumarin. At different time intervals, the media was removed, the monolayers were washed twice with PBS to remove uninternalized nanoparticles, and the cells were observed under a laser scanning confocal microscope LSM 10 (Zeiss, UK).

Cellular Drug Levels Assessment

A549 cells (passage 82) were seeded in T 75 flasks in DMEM, supplemented with sodium bi-carbonate and fetal bovine serum, at a density of 1.0×10^5 cells/flask and allowed to attach overnight. Plain drug and nanoparticles suspensions equivalent to 10^{-7} M mometasone furoate were added to the labeled wells. Untreated cells and blank nanoparticles treated cells were used as controls. The medium was changed on day 2 and no further dose of the drug was added. At different time intervals, the media from the flasks was removed and the cells washed twice with PBS to remove uninternalized nanoparticles and free drug, and the cells were lysed by incubating them with distilled water for 30 min. A portion of the cell lysates was used to determine the total amount of cell protein using Bichinconinic acid–protein assay method. The total amount of drug (free and entrapped in nanoparticles) was extracted from the cell lysates with methylene chloride and the methylene chloride was evaporated. The residue was reconstituted with the mobile phase, centrifuged and injected into the HPLC column for determination of the drug content.

Antiproliferative Studies

A549 cells (passage 82) were seeded in 24-well plates in Dulbecco's Modified Eagle medium, supplemented with sodium bi-carbonate and fetal bovine serum, at a density of 1.0×10^5 cells/well. The cells were allowed to attach overnight. Plain drug and nanoparticles suspensions equivalent to 10^{-7} M mometasone furoate were added to the labeled wells. Untreated cells and blank nanoparticles treated cells were used as controls. The medium was changed on day 2 and no further dose of the drug was added. At different time intervals, the media from the wells was removed and the cells washed twice with Hank's balanced salt solution. Fluorescein diacetate solution (100 μl of 1 μg/ml) was added to each well and incubated for 30 min. Fluorescein diacetate was washed from the cells with Hank's balanced salt solution and the cells were lysed by incubating them with distilled water for 30 min. The cell lysates were centrifuged and the amount of fluorescein (17) in the supernatant was determined using spectrofluorophotometer (RF-540, Shimadzu, Japan) at an excitation wavelength of 490 nm and emission wavelength of 512 nm. The data were recorded with data recorder (DR-3, Shimadzu, Japan).

Cell Cycle Analysis

The distribution of DNA in the cell cycle was studied by flow cytometry. A549 cells were seeded at a density of 1×10^6 cells per 2 ml in a 35 mm petri dishes and allowed to attach overnight. Plain drug or suspension of drug-loaded nanoparticles and WGA-nanoparticles equivalent to 10^{-7} M mometasone furoate was added to the cells. Blank nanoparticles-treated cells and untreated cells were used as controls. The medium was changed after 24 h, and no further dose of the drug was added. After 48 h, cells were washed twice with PBS, trypsinized, and fixed with ethanol at 4°C till analyzed. Later the cells were stained with propidium iodide and the cellular DNA content was analyzed with a fluorescent activated cell sorter (FACS, flow cytometer) to create histograms of cell frequency *versus* propidium iodide fluorescence intensity.

Mometasone Furoate HPLC Assay

The drug content was determined using a Dionex HPLC system (Dionex Softron GmbH, Germany). The HPLC system was composed of a pump (P-680, Dionex), a simple 10-μl loop injector (Reodyne 7125) and a UV-visible spectrophotometric detector (UVD 170U, Dionex).The separation

Table I. Influence of Conjugation on Particle Behavior

Formulation	Mean Particle Size (nm)	Zeta Potential (mV)	Entrapment Efficiency (%)
MF-NPs	255±7 nm	−15.3±1.9	78±5.5
WGA-MF-NPs	340±5 nm	−2.59±2.1	60±2.5

(Mean±S.D., $n=3$)
MF-NPs Mometasone furoate nanoparticles; *WGA-MF-NPs* WGA conjugated mometasone furoate nanoparticles

was carried out on a 14 cm Kromasil C 18 150-4.6 HPLC column (Merck) having particle size of 5 μm. Mobile phase for mometasone furoate consisted of a methanol and water (65:35) mixture. Diluting solution composition was methanol/water/acetic acid, (65:35:0.2). The run time of the assay was 25 min and the retention time of mometasone furoate was 16 min. During the assay, mometasone furoate was eluted isocratically at a mobile phase flow rate of 1 ml/min and monitored with a detector operating at 254 nm. Chromatographic runs were performed at room temperature and the data was analyzed using Chromeleon 6.5 software.

RESULTS AND DISCUSSION

MF furoate loaded nanoparticles were prepared by emulsion–solvent evaporation technique. The drug/polymer ratio was optimized based on entrapment efficiency and concentration of aqueous PVA solution was optimized based on drug entrapment efficiency and particle size. When concentration of PVA was increased from 0.5% to 2% *w/v*, the percent entrapment efficiency increased from to 54.5±3.5% to 83.6±2.5% and the particle size decreased from to 450±3 nm to 250±7 nm. The drop in the particle size and higher percent entrapment efficiency with the increase in PVA concentration is probably due to the differences in the stability of the emulsions formulated with different concentrations of PVA as viscosity increases with increasing PVA concentrations. It resulted in formation of a stable emulsion with smaller and uniform droplet size, leading to the formation of smaller sized nanoparticles. The percent entrapment efficiency was found to be highest with 1:2; drug/polymer ratio. Therefore, 2% *w/v* PVA solution and 1:2; drug/polymer ratio were considered as optimum for preparation of mometasone furoate nanoparticles for surface modification with WGA.

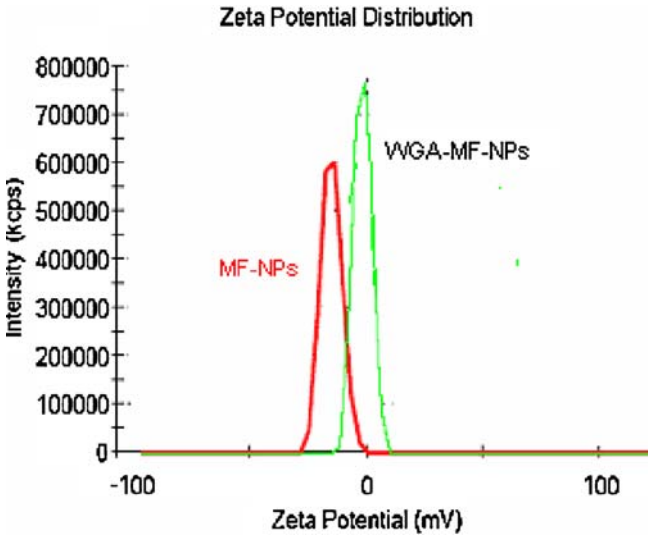

Fig. 2. Zeta potential graphs mometasone furoate nanoparticles before and after conjugation with WGA

Activation of 10 mg nanoparticles with 1.0 ml of 7.0% *w/v* solution EDAC and 1.0 ml of 0.3% *w/v* NHS solution in 20 mM HEPES/NaOH buffer, pH 7.0, and 200 μg WGA yielded WGA-nanoparticles with a lectin density of 10–15 μg/mg of nanoparticle surface.

Mean particle size and zeta potential of optimized mometasone furoate nanoparticles were found to be 255±7 nm and −15.3±1.9 mV respectively. Surface conjugation of nanoparticles by WGA altered the mean particle size, zeta potential and entrapment efficiency of the nanoparticles (Table I, Figs. 1 and 2). There was an increase in the mean particle size to 340±5 nm and the marked reduction in zeta potential from −15.3±1.9 to −2.59±2.1 due to the loss of fine particles during processing and/or presence of WGA on the surface of nanoparticles. Agglomeration tendency may have caused loss of fine particles due to cross linking of the particles by the WGA molecule containing about 24 amino groups (18). The percent entrapment efficiency of mometa-

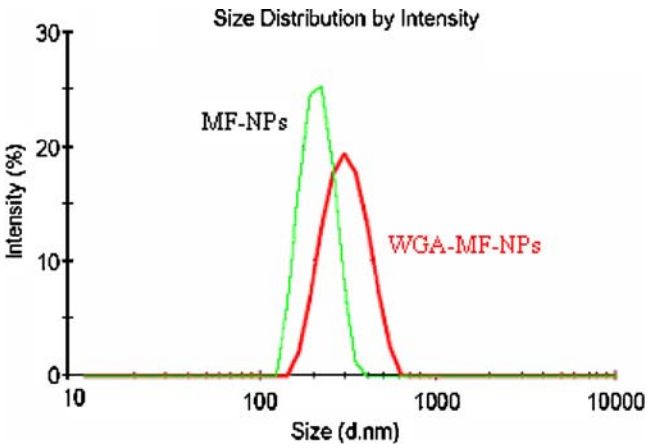

Fig. 1. Particle size distribution graphs of mometasone furoate nanoparticles before and after conjugation with WGA

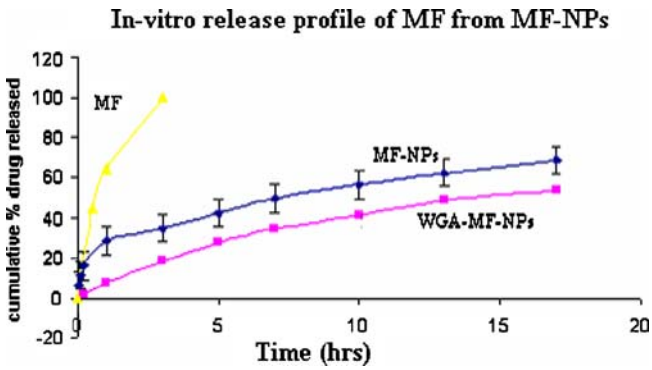

Fig. 3. *In-vitro* release of mometasone furoate from mometasone furoate nanoparticles before and after conjugation with WGA. (Mean±S.D., $n=3$)

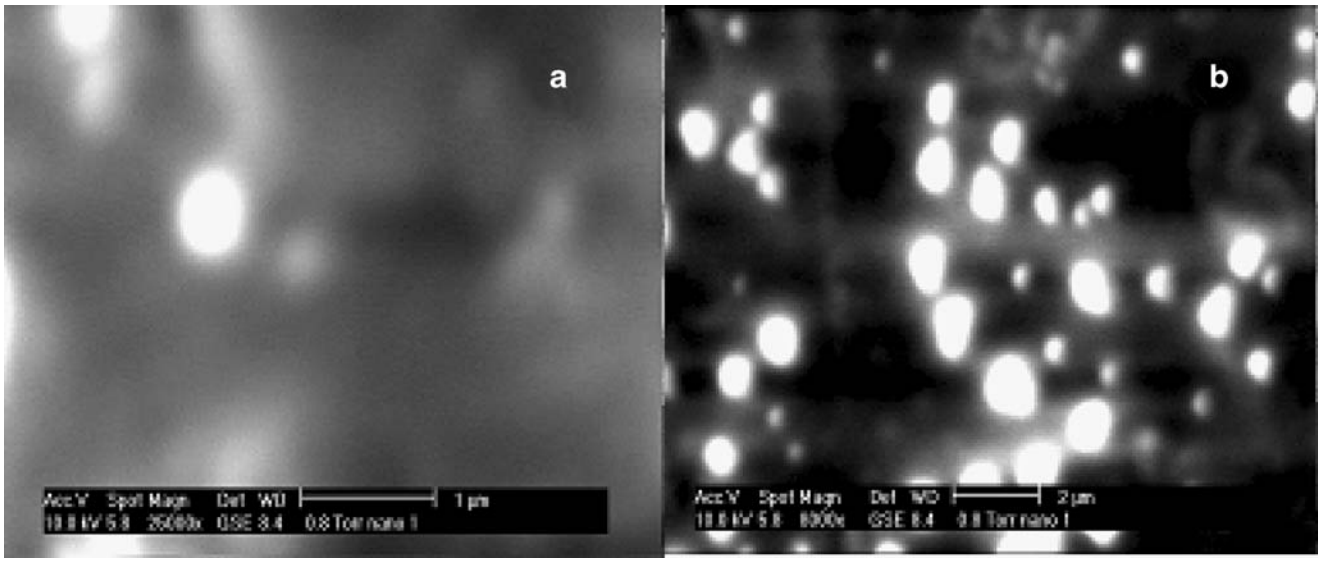

Fig. 4. ESEM showing morphology of **a** mometasone furoate nanoparticles and **b** WGA-mometasone furoate nanoparticles

sone furoate nanoparticles and WGA-mometasone furoate nanoparticles were found to be 78±5.5% and 60±2.5% respectively. The reduction in the percent entrapment efficiency may be due to the diffusion of surface drug during the conjugation process.

The release of mometasone furoate from unconjugated nanoparticles and WGA-conjugated nanoparticles into PBS (pH 7.4) was measured at 37°C. For unconjugated nanoparticles, after an initial burst release of about 25%, the release rate reduced dramatically and only 68% of the drug was released in 2 weeks. WGA-conjugated nanoparticles were devoid of any burst release. The cumulative mometasone furoate released at the end of 2 weeks was about 55% of the initial drug loading. The cumulative drug release plots of nanoparticles are plotted in Fig. 3. *In-vitro* release of mometasone furoate from plain drug was found to be 100% in 3 h. A possible reason for the absence of burst release may be absence of drug on the surface of conjugated nanoparticles and gelling of the surface WGA on contact with the release media.

The scanning electron microscopy pictures of the unconjugated and WGA-conjugated nanoparticles are shown in Fig. 4a and b. The particles appear to be spherical before and after WGA-conjugation and hence it can be deciphered that WGA-conjugation did not noticeably alter sphericity of the nanoparticles.

Confocal images at different time intervals (Fig. 5) show that the nanoparticles are taken up by the cells within 5 min of treatment with 6-coumarin loaded nanoparticles and at all time points the WGA-conjugated nanoparticles are associated to a greater extent than unconjugated nanoparticles.

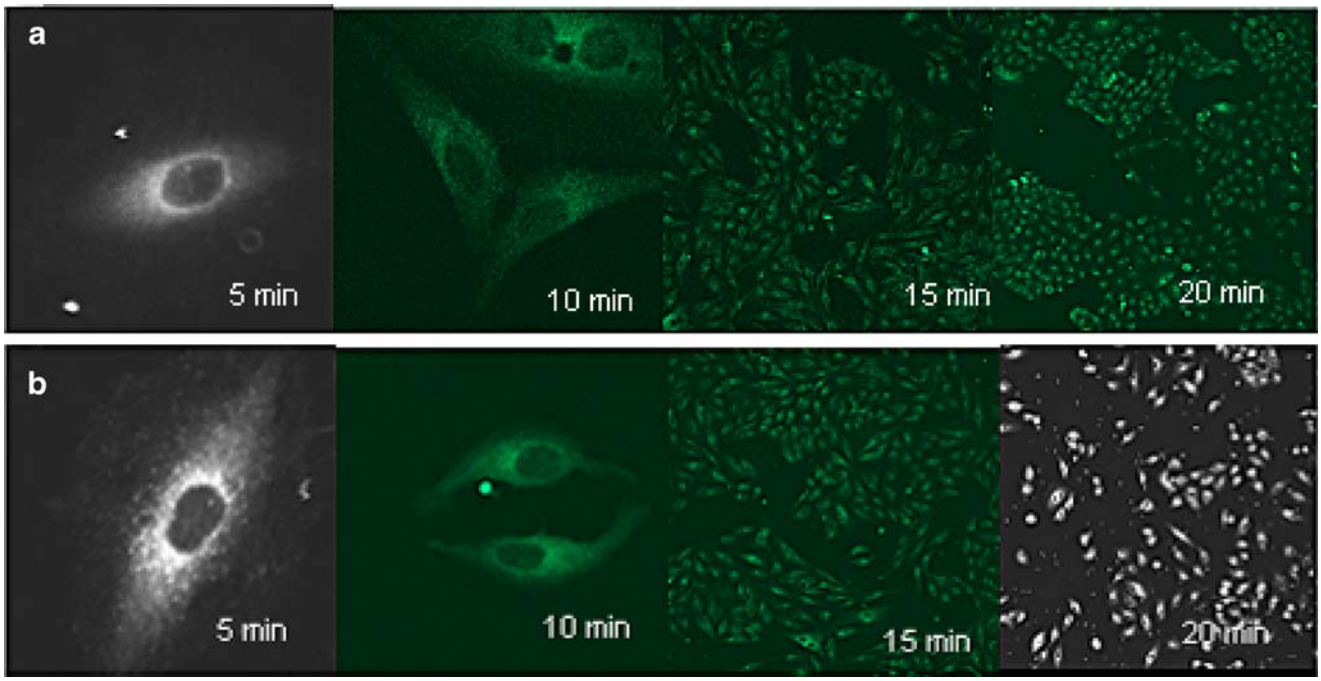

Fig. 5. Confocal images of uptake of coumarin-loaded **a** unconjugated and **b** WGA-conjugated nanoparticles after 5, 10, 15 and 20 min

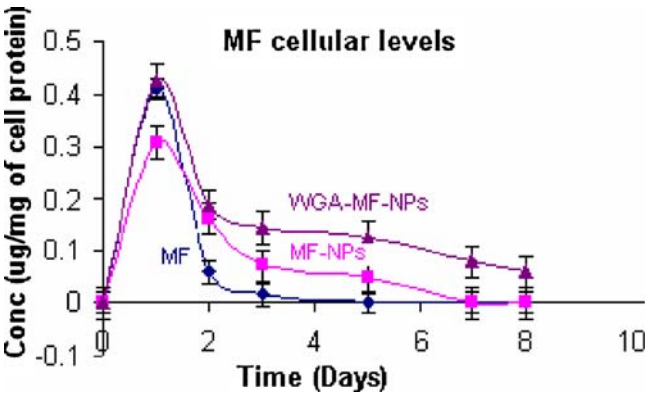

Fig. 6. Cellular mometasone furoate levels following mometasone furoate treatment (mean±S.D., $n=3$)

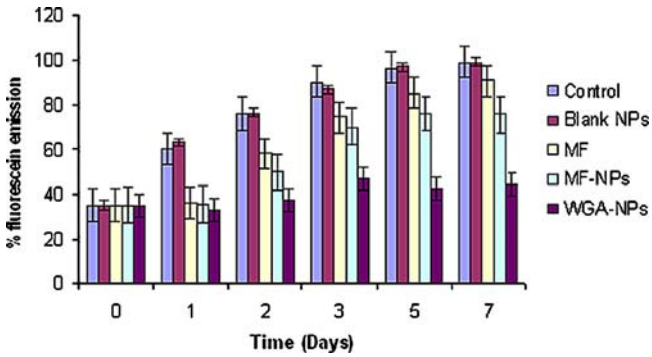

Fig. 7. Inhibition of A549 cell proliferation. Cell growth was followed by measuring the percent emission of fluorescein, the amount of which is directly proportional to the number of viable cells. (Mean±S.D., $n=3$)

Cellular drug levels were estimated at different time intervals, after treating A549 cells with plain drug, unconjugated mometasone furoate nanoparticles and WGA-conjugated mometasone furoate nanoparticles. From the cellular drug concentration–time plot (Fig. 6), increase in AUC was observed with nanoparticles than with plain drugs. Between the nanoparticles, higher AUC was observed for conjugated than for unconjugated nanoparticles. AUC was 0.4745, 0.6791 and 1.24 for plain drug, unconjugated nanoparticles and WGA-conjugated nanoparticles respectively. Cytoadhesive/cytoinvasive nature of WGA may be responsible for higher intracellular drug levels. WGA is reported to bind specifically to *N*-acetyl-D-glucosamine residues located at the surface of alveolar epithelium (7) and hence, higher uptake of conjugated nanoparticles may be reason for higher and sustained cellular drug levels.

Fluorescence diacetate **(**FDA) is a non-fluorescent molecule that passes undisturbed through the cell membranes and undergoes hydrolysis by the cell esterases (19). This results in the formation of a fluorescent substance-fluorescein (FRC). Fluorescein remains in the cytoplasm of the live cells but it diffuses out thorough the cell membrane of the dead cells. This effect is a result of the differences in the cell wall permeability for non-polar FDA and polar FRC compounds. Fluorescein intensity is directly proportional to the cell viability or number of cells. Therefore, the fluorescent intensity of the cell lysates was measured for the determining the cell proliferation. Plain drug treated cells demonstrated a transient inhibition of cell proliferation compared to untreated cells. The inhibition was seen up to 2 days following plain drug treatment. Significantly higher ($P<0.05$) and prolonged (up to 7 days) inhibition of cell proliferation was observed when cells were treated with unconjugated mometasone furoate nanoparticles and WGA-conjugated mometasone furoate nanoparticles (Fig. 7). When the results of *in-vitro* antiproliferative activities of unconjugated and conjugated MF nanoparticles were compared, increased *in-vitro* antiproliferative activity was observed with conjugated mometasone furoate nanoparticles. Blank nanoparticles did not show any inhibition when compared to untreated/control cells. Pharmacological response being directly proportional to the drug concentration, it is reasonable to believe that higher antiproliferative activity is a reflection of higher concentrations of drug available in the cytoplasm.

Cell cycle analysis was done to determine the phase of cell cycle arrest. Glucocorticoids inhibit cell growth and proliferation primarily through their effect on the cell cycle and induction of apoptosis (20) and induce cell-cycle arrest in the late G1 phase of many cell lines. While the mechanism of cell-cycle arrest in A549 cells is still not clear and could proceed through inhibition of phosphorylation of retinoblastoma protein, in lymphocytes, cell-cycle arrest proceeds through the induction of the *myc* pathway and the down-regulation of the *Bcl* gene (20). In our studies, the mechanism of inhibition of cell proliferation was found to be mediated through inhibition of cell-cycle progression with a relatively higher percentage of cells in the G0/G1 arrest phase and lower percentage of cells in the S phase in the group that was treated with drug-loaded nanoparticles compared to that treated with plain drug (Table II). Between the unconjugated and WGA conjugated NPs, a higher proportion of cells were in the G0/G1 arrest phase and lower percentage of cells in the S phase in the WGA conjugated nanoparticle treatment groups than in the group treated with unconjugated nanoparticles. Blank nanoparticles had no effect on the cell-cycle distribution, and the results were similar to the results with the untreated control. On the basis of the intracellular drug levels, it could be concluded that more drug is available at the site of action for a sustained period of time in the case of WGA-nanoparticles than in the case of the unconjugated nanoparticles and drug in solution, resulting in greater antiproliferative activity with drug-loaded nanoparticles.

Table II. Effect of Mometasone Treatments on the Cell Cycle Distribution in A549 Cells

Treatment	Percent Cells		
	G0/G1 Phase	G2/M Phase	S Phase
Untreated	70±1.3	5±0.5	24±2.5
Blank NP	70±0.9	4±1.0	26±1.9
MF	76±1.5	12±1.2	10±0.4
MF-NPs	80±0.6	11±0.8	9±0.2
WGA-MF-NPs	84±0.6	11±0.5	5±0.4

(Mean ± S.D., $n=3$)
Blank NP Blank nanoparticles; *MF* mometasone furoate; *MF-NPs* mometasone furoate nanoparticles; *WGA-MF-NPs* WGA conjugated mometasone furoate nanoparticles

CONCLUSIONS

To conclude, improved and prolonged availability and efficacy of antiasthmatic drug in alveolar epithelial cell lines after incorporation of WGA-conjugated nanoparticles was observed and hence once formulated as dry powder inhaler, it can be delivered to conducting zone of lung to alleviate common limitations in treatment of asthma such as short lived action, nocturnal exacerbations and hospitalizations of patients etc. Similar strategies may also be used in treatment of other lung disorders.

ACKNOWLEDGMENTS

The authors are thankful to the Department of Science and Technology, Government of India, for providing financial support under the Women Scientist Scheme (WOS-A).We also thank Technology Information and Forecasting Council's (TIFAC) Centre of Relevance and Excellence in New Drug Delivery System.

REFERENCES

1. H. Suh, B. Jeong, R. Rathi, and S. W. Kim. Regulation of smooth muscle cell proliferation using paclitaxel-loaded poly (ethylene oxide)-poly (lactide/glycolide) nanospheres. J. Biomed. Mater. Res. 42:331–338 (1998).
2. J. M. Anderson, and M. S. Shive. Biodegradation and biocompatibility of PLA and PLGA microspheres. Adv. Drug Delivery Rev. 28:5–24 (1997).
3. J. Panyam, and V. Labhasetwar. Biodegradable nanoparticles for drug and gene delivery to cells and tissue. Adv. Drug Deliv. Rev. 553:(3)29–347 (2003).
4. J. Panyam, W. Z. Zhou, S. Prabha, S. K. Sahoo, and V. Labhasetwar. Rapid endo-lysomal escape of poly (D,L-lactide-co-glycolide) nanoparticles: implication for drug and gene delivery. FASEB J. 16:1217–1226 (2002).
5. I. J. Goldstein, and C. E. Hayes. The lectins: carbohydrate-binding proteins of plants and animals. Adv Carbohydr Chem Biochem. 35:127–340 (1978).
6. M. A. Clark, B. H. Hirst, and M. A. Jepson. Lectin-mediated mucosal delivery of drugs and microparticles. Adv. Drug Deliv. Rev. 43(2–3):207–223 (2000).
7. R. Abu-Dahab, U. F. Schafer, and C. M. Lehr. Lectin-functionalized liposomes for pulmonary drug delivery: effect of nebulization on stability and bioadhesion. Eur. J. Pharm. Sci. 14(1): 37–46 (2001).
8. C. M. Lehr. Lectin-mediated drug delivery: the second generation of bioadhesives. J. Control Release. 65(1–2):19–29 (2000).
9. C. Crocker, Chang Yi Zhou, A. Bewtra, W. Kreutner, and R. Townley. Glucocorticosteroids inhibit leukotriene production. Ann. Allergy Asthma Immunol. 78:497–505 (1997).
10. D. J. Margolskee. Clinical experience with MK-571: a potent and specific LTD4 receptor antagonist. Ann. N. Y. Acad. Sci. 629:148–156 (1991).
11. N. Chanarin, and S. L. Johnston. Leukotrienes as a target in asthma therapy. Drugs. 47(1):12–24 (1994).
12. D. P. Skoner, L. Lee, W. J. Doyle *et al*. Nasal physiology and inflammatory mediators during natural pollen exposure. Ann. Allergy. 65:206–210 (1990).
13. B. E. Barton, J. P. Jakway, S. R. Smith, and M. I. Siegel. Cytokine inhibition by a novel steroid, Mometasone furoate. Immunopharmacol. Immunotoxicol. 13(3):251–261 (1991).
14. U. B. Kompella, N. Bandi, and S. P. Ayalasomayajula. Poly (lactic acid) nanoparticles for sustained release of budesonide. Drug Delivery Technology. 1:29–35 (2001).
15. Z. Grabarek, and J. Gergely. Zero-length cross-linking procedure with the use of active esters. Anal. Biochem. 185:131–135 (1990).
16. S. Naazneen, S. Naik, T. Bagchi, and A. Misra. Assessment of *in-vitro* antiproliferative activity after intracellular drug delivery from wheat germ agglutinin-conjugated budesonide nanoparticles. J. Biomed. Nanotechnol. 3:61–67 (2007).
17. M. Nikolova, I. Savova, and M. Marinov. An optimized method for investigation of the yeast viability by means of fluorescent microscopy. J. Cult. Collect. 3(1):66–71 (2002).
18. M. Wirth, A. Fuchs, M. Wolf, B. Ertl, and F. Gabor. Lectin mediated drug targeting: preparation, binding characteristics and antiproliferative activity of wheat germ agglutinin conjugated doxorubicin on Caco-2 cells. Pharm. Res. 15:1031–1037 (1998).
19. K. D. Wittrup, and J. E. Bailey. Comments on a segregated model of recombinant cultures. Biotechnol. Bioengineering. 35:525–532 (1990).
20. J. A. Cidlowski, K. L. King, R. B. Evans-Storms, J. W. Montague, C. D. Bortner, and F. M. Hughes Jr. The biochemistry and molecular biology of glucocorticoid-induced apoptosis in the immune system. Recent Prog. Horm. Res. 51:457–490 (1996).